JPE 15-4-15

http://dx.doi.org/10.6113/JPE.2015.15.4.1018
ISSN(Print): 1598-2092 / ISSN(Online): 2093-4718

Practical Photovoltaic Simulator with a Cross Tackling Control Strategy Based on the First-hand Duty Cycle Processing

Shuren Wang[†], Wei Jiang[*], and Zhengyu Lin[**]

[†*]School of Hydraulic, Energy and Power Engineering, Yangzhou University, Yangzhou, China
[**]School of Power Electronics and Power Systems, Aston University, Aston, U.K.

Abstract

This paper proposes a methodological scheme for the photovoltaic (PV) simulator design. With the advantages of a digital controller system, linear interpolation is proposed for precise fitting with higher computational efficiency. A novel control strategy that directly tackles two different duty cycles is proposed and implemented to achieve a full-range operation including short circuit (SC) and open circuit (OC) conditions. Systematic design procedures for both hardware and algorithm are explained, and a prototype is built. Experimental results confirm an accurate steady state performance under different load conditions, including SC and OC. This low power apparatus can be adopted for PV education and research with a limited budget.

Key words: Cross tackling control, Open circuit (OC), Photovoltaic (PV) simulator, Power conversion, Short circuit (SC)

I. INTRODUCTION

People around the world are confronted with the shortage of conventional energy resources and environmental problems caused by the excessive reliance on fossil fuels. Photovoltaic (PV) systems enable a zero-emission and renewable electricity harvesting method. PV panels gained worldwide acceptance and extensive application because it has a long life-time operation and no moving parts; PV panels are environment-friendly and nearly maintenance-free [1]-[3]. PV modules possess non-linear V-I output characteristics with several factors (e.g. temperature and irradiance), hence interfacing conditioners with maximum power point tracking (MPPT) are required to get energy from PV panels with improved efficiency. A number of MPPT algorithms were studied theoretically and experimentally in the past decade. However, field tests with real PV panels are sometimes unpredictable because of various factors [4], [5]. With a PV simulator that emulates the V-I output characteristic of an actual PV module, testing the PV powered system became repeatable and durable; testing can be conducted at any time and under any weather condition [6].

A PV simulator conceptually consists of a simulating core to produce the V-I characteristic standard value, power amplifying stages, and local controller. In the literature, three main approaches are chosen to design a simulating core. One of the approaches is the use of actual mini PV cells or photo diodes with a controllable illuminant [7]-[9]. Apparently, this method changes the irradiant condition such as partial shading or different sunlight. However, determining the influence of other factors (e.g. temperature) on the output characteristic is difficult and expensive. Another method uses mixed circuits that are patterned after a PV cell [10]-[14]. In the mixed circuit design, output characteristics can manually toggled by triggering functional blocks in the circuits. The digital implementation of the simulating core is becoming popular because it has more high-performance microcontrollers. The V-I output reference value can be directly calculated from the physical equations in the running program. A lookup table can also be made beforehand. Furthermore, the online modification can be achieved using data communication with a computer. In this paper, a DC/DC converter-based PV simulator is designed

Manuscript received Dec.. 11, 2014; accepted Mar. 18, 2015
Recommended for publication by Associate Editor Woo-Jin Choi.
[†]Corresponding Author: jiangwei@yzu.edu.cn
Tel & Fax: +86-051487971315, Yangzhou University
Department of Electrical Engineering, Yangzhou University, China.
[*]School of Hydraulic, Energy and Power Engineering, Yangzhou University, Yangzhou, China
[**]School of Power Electronics and Power Systems, Aston University, Aston, U.K.

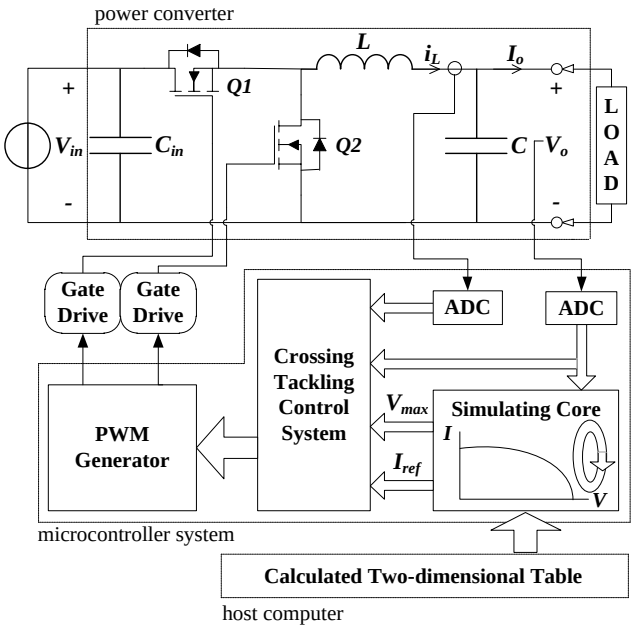

Fig. 1. System structure.

that enables the customization of the output characteristic of the PV simulator according to the target PV modules and its operation conditions.

Most conventional designs fail to consider short circuit (SC) and open circuit (OC) operation states in the literature, even though SC and OC are two common operation states for PV modules in practical missions. A high-performance PV simulator can work in both SC and OC states. To ensure the ideal working points for a PV simulator under SC and OC cases, a cross tackling control strategy is proposed.

For PV simulator testing, resistive loads are commonly chosen to verify whether the simulator follows the non-linear V-I curve of the real PV modules. Constant current loads are also used [8], [15]. However, most practical MPPT technologies force the voltage of input power source to be constant in steady states [16]-[18]. In this paper, a constant voltage load is used to run the functional test.

Commercially-available PV simulators are expensive because of the high power rating [13]. Affordable PV simulators with a low power rating are also essential for the MPPT algorithm verification with limited budget. The proposed design is useful for some research activities in small laboratories and teaching exercises in schools.

II. System Description

As shown in Fig. 1, the proposed system is mainly composed of three sections: DC/DC power converter, microcontroller system, and host computer. A synchronous buck topology is used for enhanced efficiency, thus the converter produces voltage ranging from 0 to V_{in}. The power converter is designed such that the output voltage V_o and inductor current i_L follows the V-I curve. The host computer configures a customized curve and computes an array table.

Output voltage, V_o, is identified and used as input to the simulating core. After generating a table look-up, a current reference value I_{ref} is produced according to the V-I curve. The calculation result of the simulating core I_{ref} together with the maximum output voltage of actual PV module (simulation target) V_{max} are used as reference values for the current control subsystem and voltage control subsystem, respectively. The output is processed by the crossing tackling control system.

A detailed control strategy will be discussed in Section V. A corresponding duty cycle is calculated by the controller; two complementary PWM signals with a dead-time are generated to drive Q1 and Q2.

III. Implementation of Simulating Core

To follow the actual PV output characteristic, a mathematical model of the PV output characteristic is introduced and an algorithm is presented.

Different mathematical models are proposed to present the non-linear PV characteristic. If the parameters of the PV array are detailed enough, a circuit model is drawn and the output V-I equation is calculated considering environmental factors (e.g. temperature and illumination) [19]. A set of formulas are commonly derived to describe the non-linear V-I characteristic, and this calculation method only requires four parameters [4, 20]. Maximum power point voltage (V_{mp}), maximum power point current (I_{mp}), open circuit voltage (V_{oc}), and short circuit current (I_{sc}) are four available parameters of commercial PV module products. In the proposed design, a 100W PV module is used as the simulation target, and V_{mp} (18V), I_{mp} (5.55A), V_{oc} (21.6V) and I_{sc} (6.11A) are measured at 25ºC and 1000W/m^2 irradiance. With the V-I equation set, a V-I curve under a specific condition (assuming it is under 25 ºC and 1000W/m^2 irradiance) is drawn in Fig. 2. For digital use, array elements that indicate operation points of the curve are calculated from V-I equations using the computer and saved in the microcontroller. Different PV modules or one under different generating conditions are calculated and simulated by digitizing the curve data without exceeding the power rating. Using more data points results in a finer V-I curve. However, it is impractical to save hundreds of elements into the controller to match every practical value of V_o. In this design, a 30-point, two-dimensional table is used with concentrated data near the expected maximum power points.

To get the theoretical output reference value I_{ref} from the two-dimensional table with practical voltage V_o, a table lookup method combined with the piecewise linear interpolation is designed. Piecewise interpolation entails curve fitting using different polynomials in various curve

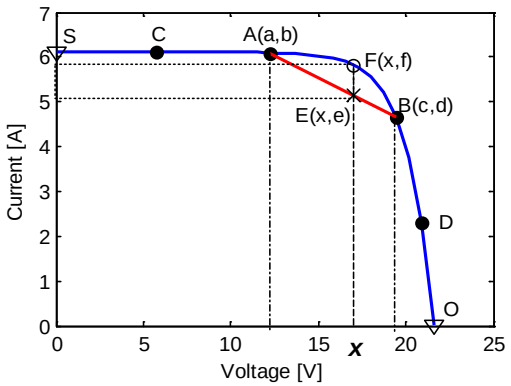

Fig. 2. V-I curve and piecewise linear interpolation method.

segments. Linear polynomials are preferred because of reduced computation load. In the simulating core, the digital value of the output voltage V_o is used as an index for look-up and interpolation calculation. Assuming that the V-I curve in Fig. 2 is divided into five segments by six points (A, B, C, D, S and O)., point A (a, b) and point B (c, d) are two adjacent fixed points. Two possible cases should be discussed. In one case, V_o is equal to a or c, thus the look-up program can directly find the result from the array and corresponding data b or d that indicate the theoretical current reference value will be obtained. Accordingly, the simulator is working at point A or B. In other instances, V_o is equal to x, and I_{ref} should be f. For the linear interpolation method, line segment AB represents curve segment AFB. The equation of line segment AB is

$$y = b + (d - b)\frac{x - a}{c - a} \tag{1}$$

When V_o is x, a mathematical calculation value e is obtained from Equation (1) because point E is the matching point in segment AB. Consequently, I_{ref} is equal to e that is the approximate value of f. After the processing the control, the simulator works at point E instead of the ideal power point F. Apparently, an error exists when piecewise linearization is used for the nonlinear V-I curve. The concentrated data point near the maximum power point reduces the error substantially.

IV. System Design and Control Strategy

A. Hardware Design

Circuit elements and their values are prepared for a prototype design.

As shown in Fig. 1, the power stage of the system is a buck converter with an input voltage V_{in} of 30V. Input capacitor C_{in} is used to reduce the input current ripple. For Q1 and Q2, a 500ns dead-time is introduced in the PWM generator to prevent cross conduction. The inductor current I_L is always continuous because the negative current is allowed for the synchronous buck. Hence inductor value L is calculated by

TABLE I
Parameters of the Circuit Elements

Element	Parameter
V_{in}	30V
C_{in}	20μF
f_s	100kHz
f_{AD}	20kHz
L	50μH
C	60μF
R_{ESR}	50mΩ

$$L = \frac{D(1-D)V_{in}}{\Delta i_L f_s} \tag{2}$$

Capacitor C is used to smoothen the output voltage by absorbing the current ripple. The LPF formed by L and C is essential for the design, and C is calculated by

$$C = \frac{(1-D)V_o}{8\Delta V_o L f_s^{\,2}} \tag{3}$$

The microcontroller system in Fig. 1 mainly consists of a microchip 16-bit digital signal controller (DSC) dsPIC33FJ64GS606 which runs at 40MHz. Linear current sensor ACS711 of Allegro MicroSystems is used to measure I_L, and two ADCs of the DSC are configured to measure V_o and I_L. The converter operates at a 100 kHz-switching frequency and 20 kHz-sampling frequency. The DC resistance of inductor R_L and ESR of output capacitor R_{ESR} are also taken into consideration.

The designed system parameters are shown in Table I.

B. Current Mode Control

Current mode control is a major part of this simulator. It forces the power circuit to produce a controllable current based on the output voltage. To ensure a controllable output current, inductor current control is designed. The converter, current sensor, and ADC are analyzed for control precision.

The inductor current control system block diagram is shown in Fig. 3. In a current control loop, the digital value I_{ref} is generated by the simulating core based on the real-time output voltage V_o. It is compared with the measured inductor current I_L. The plant represents the buck converter and $G_{id}(s)$ is the small signal transfer function between the inductor current and duty cycle in Equation (4).

$$G_{id}(s) = \frac{\tilde{i}_L(s)}{\tilde{d}(s)} = \frac{(1 + (R + R_{ESR})Cs)V_{in}}{LC(R + R_{ESR})s^2 + (L + CR_{ESR}R_L + CR(R_{ESR} + R_L))s + R + R_L} \tag{4}$$

In Equation (4), R is the load of the converter and G_{id} is only changed with load. Short circuit (SC, R=0), maximum power point output (MPP, R=V_{mp}/I_{mp}), and open circuit (OC, R=∞) are three especial operation states in system operation. However, working under OC state (point O in Fig. 2) is not feasible for current mode control because of the insignificant

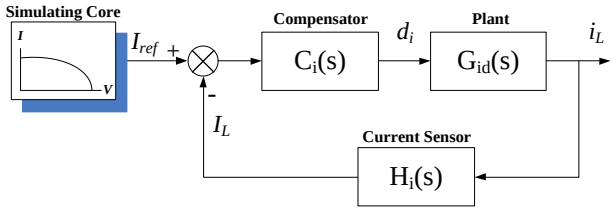

Fig. 3. Block diagram of the inductor current control system.

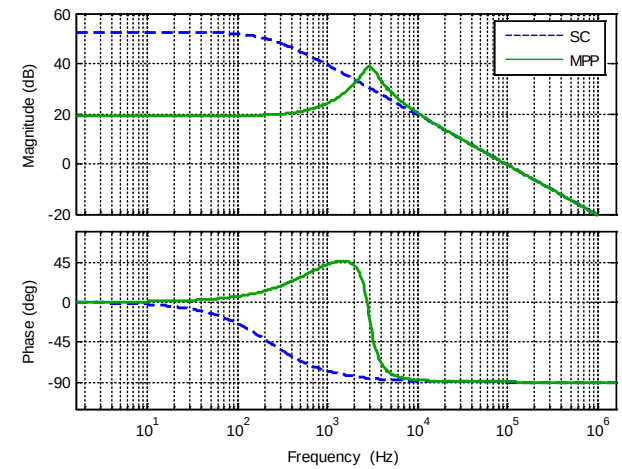

(a)

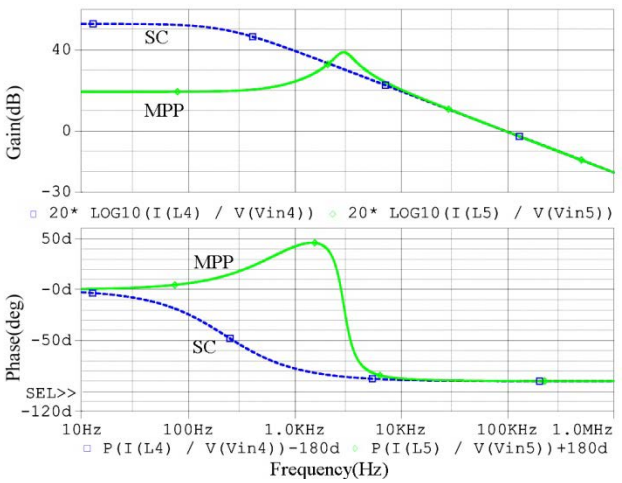

(b)

Fig. 4. Transfer function of G_{id}. (a) Bode plot of $G_{id.}$ from Equation (4). (b) Bode plot of $G_{id.}$ from the simulation.

current. The control mode under OC state will be discussed in detail. Load R is assumed to be 0.01Ω at the SC condition that facilitates the control system analysis. After substituting the values of the circuit parameters, $G_{id}(s)$ under these two states (SC and MPP) are calculated and bode plots of the transfer function in Equation (4) are shown in Fig. 4(a). A PSPICE simulation is used to verify Equation (4). Taking advantage of AC sweep, the gain from the duty cycle to the inductor current is illustrated in Fig. 4(b).

$H_i(s)$ is the transfer function of the current sensor ACS711. According to the characteristic performance of ACS711, time-domain parameters are calculated. The transfer function

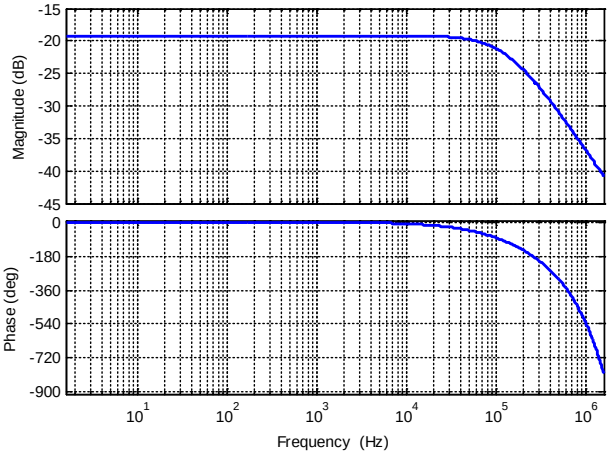

Fig. 5. Bode plot of H_i.

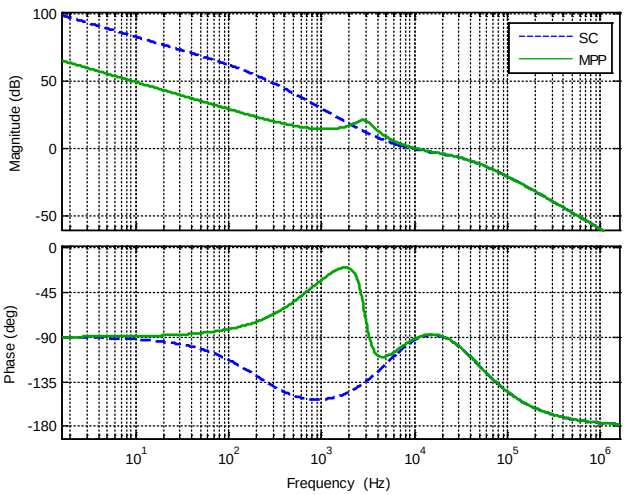

Fig. 6. Bode plot of the compensated current control system.

with a time delay factor $H_i(s)$ is derived by

$$H_i(s) = \frac{0.11}{1.2\times10^{-6}\cdot s+1} e^{-1.25\times10^{-6}\cdot s} \quad (5)$$

The bode plot of current sensor ACS711 is shown in Fig. 5.

Considering both stability and quick response, a Type 3 amplifier is designed. A bode plot of the compensated current system in SC and MPP states are shown in Fig. 6.

A discrete-time equivalent is obtained using the Tustin method. With the digital current compensator, a stable current control system is obtained. Consequently, the current mode control is capable of operating on both states except in points near the OC state.

C. Cross Tackling Control Strategy

The PV module acts like a constant voltage source in a high-voltage region (e.g. curve segment DO in Fig. 2). In fact, PV output voltage also slightly varies in this region. Fortunately, current mode control still works in this region as long as more dots are used for the table looking-up. Hence, in most cases, the regulated output voltage is generated by an output current control instead of a direct output voltage

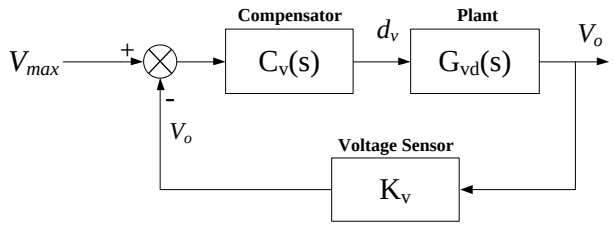

Fig. 7. Block diagram of output voltage control system.

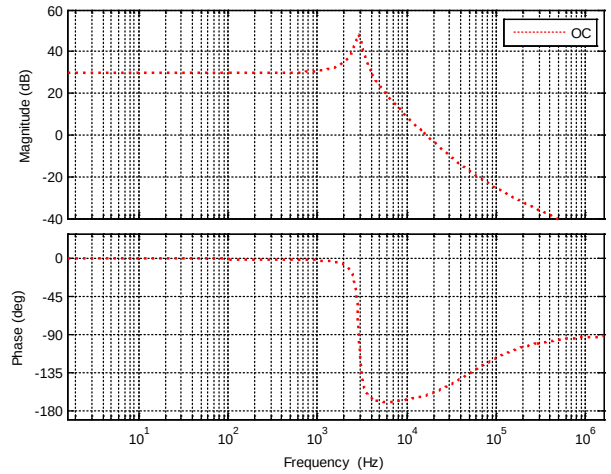

(a)

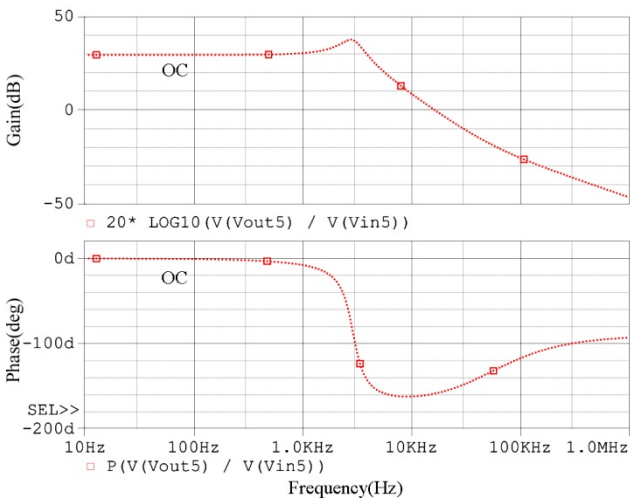

(b)

Fig. 8. Bode plot of G_{vd}. (a) Bode plot of G_{vd} from Equation (6). (b) Bode plot of G_{vd} from the simulation.

control. A current mode subsystem is sufficient for a routine simulating state.

However, if the load is significantly light and acts as a constant voltage that is larger than V_{oc} (21.6V for this simulating target), current mode control is not a good choice because error during sampling may destabilize the control effort. A single current mode control cannot guarantee good tracking performance in a light load region. Therefore, an improved control strategy involving the voltage control loop

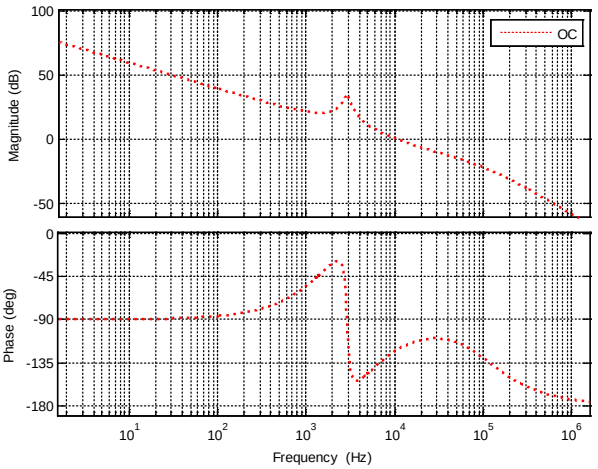

Fig. 9. Bode plot of the compensated voltage control system.

is needed.

The output voltage control subsystem block diagram is shown in Fig. 7. V_{max} is a digital value indicating the maximum voltage of the simulation target (V_{oc}). V_{max} is the chosen reference value of the voltage loop to keep the output voltage equal to V_{oc}. The plant represents the buck converter, and $G_{vd}(s)$ is the small signal transfer function between output voltage and duty cycle and is obtained by

$$G_{vd}(s)=\frac{\tilde{v}_C(s)}{\tilde{d}(s)}=\frac{(1+RR_{ESR}Cs)RV_{in}}{LC(R+R_{ESR})s^2+(L+CR_{ESR}R_L+CR(R_{ESR}+R_L))s+R+R_L} \quad (6)$$

R is the load of the converter and G_{vd} is changed alone with R. The voltage mode control is designed for an OC state or other light load states; hence R=1000 Ω is calculated using Equation (6) for an approximate analysis. G_{vd}, under light load state (R=1000Ω) is calculated and bode plots of the transfer function Equation (6) are shown in Fig. 8(a). A PSPICE simulation work is performed to verify the model in Equation (6). Taking advantage of the AC sweep, the gain from duty cycle to the inductor current is illustrated in Fig. 8(b).

A compensator, $C_v(s)$, is designed based on the system characteristic. The bode plot of the compensated voltage control loop at OC is shown in Fig. 9. As a result, the output voltage remains as V_{oc} during the voltage control loop working.

With the current control loop and voltage control loop, a cross tackling control strategy that runs the simulator in every practical load case is proposed. The algorithm that directly deals with the duty cycle is shown on Fig. 10. Variables d_i and d_v are the calculated results of the current control loop and voltage control loop, respectively. Variable d is the final duty cycle that is used by the PWM generator. The converter first handles two output duty cycles, d_v and d_i, and chooses the minimum value for final use. Instead of using a convenient double loop control algorithm, the proposed strategy tackles both voltage mode control and current mode

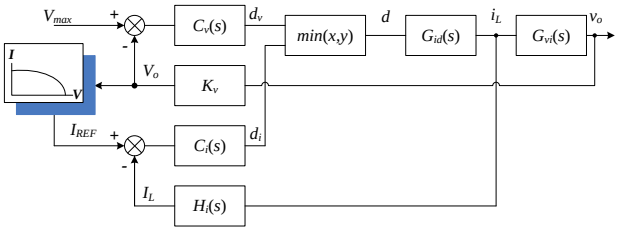

Fig. 10. Block diagram of the cross tackling control algorithm.

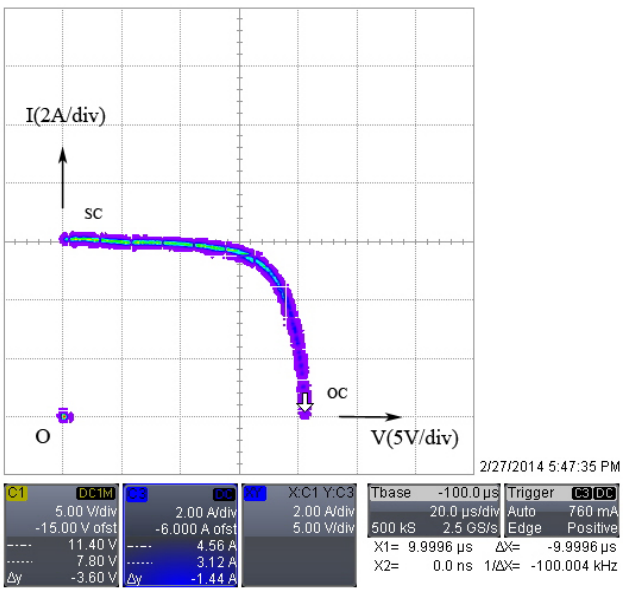

Fig. 11. V-I curve with a constant voltage load.

control by choosing a duty cycle. Switching from one mode to the other is sustained, depending on the load state during that particular moment. Conceptually, the output voltage of the buck converter is directly proportional to the duty cycle D based on the equation

$$D = \frac{V_o}{V_i} \tag{7}$$

There is always a fixed duty cycle corresponding to the V_{oc} for a certain PV module. The voltage control loop provides an amplitude restriction for each simulation target.

V. Experimental Results

A power source prototype is built based on the methods discussed earlier. An electronic load which was chosen as the load works at a constant voltage mode, and the voltage increases from 0V to 24V with a step size of 0.4V per second. Every operation point of this process is recorded by the oscilloscope, as shown in Fig. 11. The horizontal axis is the output voltage and vertical axis indicates the output current. As the voltage generated by the electronic load changes, the simulator tracks the ideal V-I curve effectively, including the SC and OC points, and a continuous transition is achieved.

The voltage-power (V-P) curve of the simulator is shown in Fig. 12. The maximum power is achieved at 100W at the

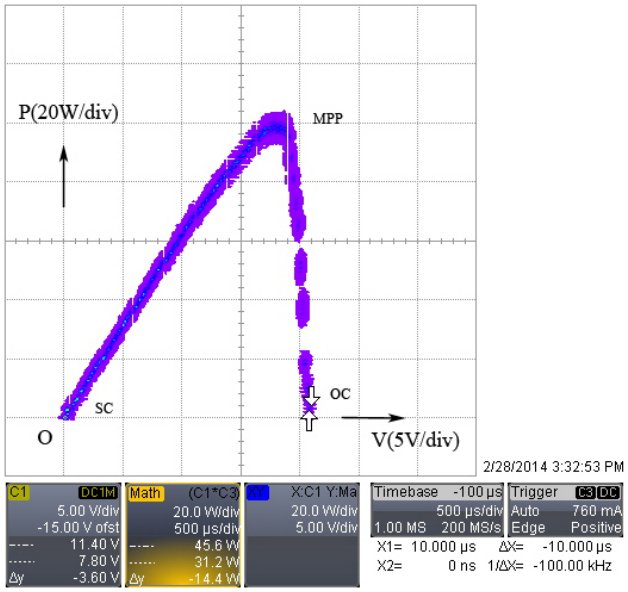

Fig. 12. V-P curve with a constant voltage load.

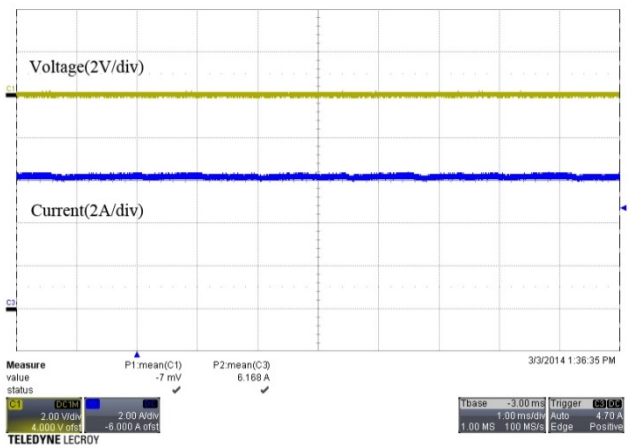

Fig. 13. Waveform of simulator under the SC state.

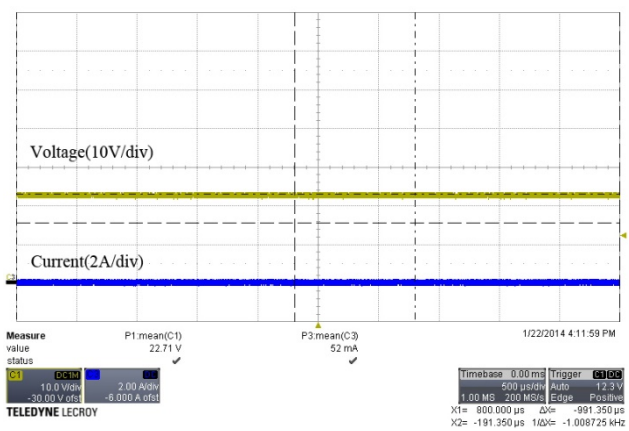

Fig. 14. Waveform of simulator under the OC state.

MPP condition. Two 0W points are also achieved in the SC and OC points. These results prove that a more practical and ideal I-V curve can be obtained with this simulator control strategy.

The simulator performance under the SC and OC states are

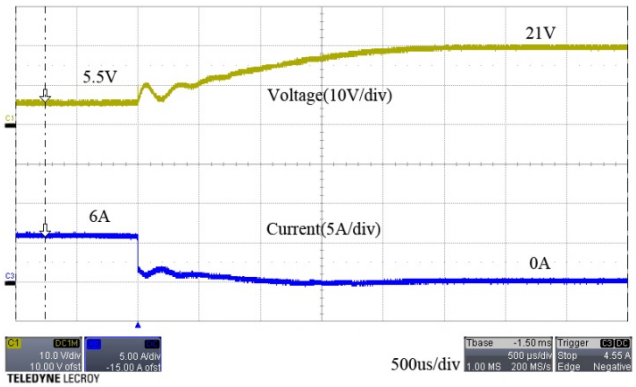

Fig. 15. Transition from the current mode to voltage mode.

shown in Fig. 13 and Fig. 14. The excellent waveforms are produced under SC and OC. Fig 15 illustrates the transient from the current mode to the voltage mode that works at the OC state. A continuous process is achieved because an increasing duty cycle is applied.

VI. Conclusions

A digital PV simulator is proposed and the design procedure is described in this paper. The interpolation method is introduced for the inner curve fitting of the simulating core instead of the single table lookup method. A prototype is built based on the control system analysis. A cross tackling control strategy that depends on both current control loop and voltage control loop is proposed for every operation state, including two extreme working states (OC and SC).

Experimental results illustrate minimal difference between the ideal PV and the simulated output characteristic. Constant current during SC and constant voltage during OC are successfully achieved.

PV simulators are useful apparatuses with the development of the PV industry. More reliable, available, and effective products are in demand. With a novel design scheme, this simulator proven to be suitable for teaching and laboratory research applications.

Acknowledgment

This work is sponsored by the National Natural Science Foundation of China (grant number 51207135), Jiangsu Natural Science Foundation (grant number BK2012266), and YZU-Yangzhou City Joint Fund (grant number 2012038-10) , CSC No. 201409300007.

References

[1] M. Shahidehpour and F. Schwartz, "Don't let the sun go down on PV," *IEEE Power Energy Mag.*, Vol. 2, No. 3, pp. 40-48, May/Jun. 2004.

[2] A. Tariq and M.S. J. Asgha, "Development of an analog maximum power point tracer for photovoltaic panel," in *Proc. IEEE Power Electronics and Drives Systems*, Vol. 1, pp. 251-255, 2005.

[3] H. Mekki, A. Mellit, H. Salhi, and B. Khaled, "Modeling and simulation of photovoltaic panel based on artificial neural networks and VHDL-language," in *Proc. 14th IEEE Int. Conf. Electron., Circuits Syst. (ICECS)*, pp. 58-61, 2007.

[4] K. Khouzam, C. Khoon Ly, C. Koh, and P. Y. Ng, "Simulation and real-time modelling of space photovoltaic systems," in *Proc. IEEE 1st World Conf. Photovoltaic Energy Convers., Conf. Record 24th IEEE Photovoltaic Spec. Conf.*, Vol. 2, pp. 2038-2041, 1994.

[5] Q. Zeng, P. Song, and L. Chang, "A photovoltaic simulator based on dc chopper," in *Proc. IEEE CCECE Conf.* Vol. 1, pp. 257-261, 2002.

[6] S. Ldloyd, G. Smith, and D. Infield, "Design and construction of a modular electronic photovoltaic simulator," in *Proc. Inst. Electr. Eng. Power Electr. Variable Speed Drives Conf.*, pp. 120-123, 2000.

[7] S. Armstrong, C. Lee, and W. Hurley, "Investigation of the harmonic response of a photovoltaic system with a solar emulator," in *Proc. Eur. Conf. Power Electron. Appl.*, pp. 1-8, 2005.

[8] O. Midtgard, "A simple photovoltaic simulator for testing of power electronics," in *Proc. Eur. Conf. Power Electron. Appl.*, pp. 1-10, 2007.

[9] A. Koran, K. Sano, R. Kim, and J. Lai, "Design of a photovoltaic simulator with a novel reference signal generator and two-stage LC output filter," *IEEE Trans. Power Electron.*, Vol. 25, No. 5, pp. 1331-1338, May 2010.

[10] J. Ollila, "A medium power PV-array simulator with a robust control strategy," in *Proc. IEEE Conf. Control Appl.*, pp. 40-45, 1995.

[11] P. Marenholtz, "Programmable solar array simulator," *IEEE Trans. Aerosp. Electron. Syst.*, Vol. AES-2, No. 6, pp. 104-107, Nov. 1966.

[12] L. Yongdong, R. Jianye, and S. Min, "Design and implementation of a solar array simulator," in *Proc. ICEMS Int. Conf.*, pp. 2633-2636, 2004.

[13] Schofield, D.M.K., Foster, M.P., Stone, D.A., "Low-cost solar emulator for evaluation of maximum power point tracking methods," *Electronics Letters*, Vol. 47, No. 3, pp. 208-209, Feb. 2011.

[14] A. Koran, T. LaBella, and J. Lai, "High Efficiency Photovoltaic Source Simulator with Fast Response Time for Solar Power Conditioning Systems Evaluation," *IEEE Trans. Power Electron.*, Vol. 29, No. 3, pp. 1285-1297, Mar. 2014.

[15] J. Zhao and J. W. Kimball, "A Digitally Implemented Photovoltaic Simulator with a double current mode controller," in *Proc. Appl. Power Electron. Conf. (APEC)*, pp. 53-58, Feb. 2012.

[16] E. Koutroulis, K. Kalaitzakis, and N. Voulgaris, "Development of a microcontroller-based, photovoltaic maximum power point tracking control system," *IEEE Trans. Power Electron.*, Vol. 16, No. 1, pp. 46-54, Jan. 2001.

[17] Y. Chen and K. Smedley, "A cost-effective single-stage inverter with maximum power point tracking," *IEEE Trans. Power Electron.*, Vol. 19, No. 5, pp. 1289-1294, Sep. 2004.

[18] M. Fortunato, A. Giustiniani, G. Petrone, G. Spagnuolo, and M. Vitelli, "Maximum power point tracking in a one-cycle-controlled single-stage photovoltaic inverter," *IEEE Trans. Ind. Electron.*, Vol. 55, No. 7, pp. 2684-2693,

Jul. 2008.
[19] C. Hua, J. Lin, and C. Shen, "Implementation of a DSP-controlled photovoltaic system with peak power tracking," *IEEE Trans. Ind. Electron.*, Vol. 45, No. 1, pp. 99-107, Feb. 1998.
[20] M. G. Villalva, J. R. Gazoli, and E. R. Filho, "Comprehensive approach to modeling and simulation of photovoltaic arrays," *IEEE Trans. Power Electron.*, Vol. 24, No. 5, pp. 1198-1208, May 2009.

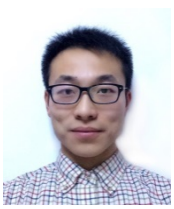

Shuren Wang was born in Yantai, China, in 1990. He received his BSEE degree from the School of Energy and Power Engineering, Yangzhou University, Yangzhou, China in 2013. He is currently working on his M.S. degree in Electrical Engineering at Yangzhou University. He is engaged in research on power electronics and control, including electronic load, DC/DC converters, matrix converters, and the application of power electronics in renewable energy systems. DC motor control is also one of his interests.

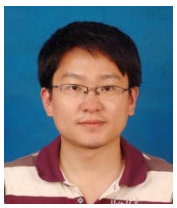

Wei Jiang was born in Yangzhou, China, in 1980. He received his B.S. degree from Southwest Jiaotong University, Chengdu, China, in 2003, and M.S. and Ph.D. degrees in Electrical Engineering from the University of Texas at Arlington, Texas, Arlington in 2006 and 2009, respectively. From 2007 to 2008, he worked in EF Technologies L.L.C. as a senior design engineer. In 2010, he joined Yangzhou University as a lecturer and founded Smart Energy Laboratory, where he is an associate professor. Currently, he is on sabbatical leave in the University of Strathclyde, Glasgow, UK, as a visiting professor. His current research interests include digitalized power conditioning to renewable energy and energy storage devices and microscopic analysis of electromechanical energy conversion.

Zhengyu Lin was born in China in 1976. He received his B.Sc. and M.Sc. degrees from the College of Electrical Engineering, Zhejiang University, Hangzhou, China, in 1998 and 2001, respectively, and t Ph.D. degree from Heriot-Watt University, Edinburgh, UK in 2005. He is currently a Lecturer with Electrical, Electronic and Power Engineering, Aston University, Birmingham, UK. He was a Research Associate at the University of Sheffield, Sheffield, UK, from 2004 to 2006, R&D Engineer in Emerson Industrial Automation, Control Techniques PLC, from 2006 to 2011, Senior Research Scientist in Sharp Laboratories of Europe Ltd. from 2011 to 2012, and lecturer at Coventry University, Coventry, UK, from 2013 to 2014. His research interests include power electronics and its applications in renewable energy, energy storage, motor drives, and power systems.